resources

MDPI

Article

Evaluation of Wetland Area Effects on Hydrology and Water Quality at Watershed Scale

Dipesh Nepal [1], Prem Parajuli [1,*], Ying Ouyang [2], Filip To [1], Nuwan Wijewardane [1] and Vivek Venishetty [1]

[1] Department of Agricultural and Biological Engineering, Mississippi State University, Mississippi State, MS 39762, USA; dn590@msstate.edu (D.N.)
[2] Center for Bottomland Hardwoods Research, USDA Forest Service, Mississippi State, MS 39762, USA
* Correspondence: pparajuli@abe.msstate.edu

Abstract: Change in land use and land cover (LULC) is crucial to freshwater ecosystems as it affects surface runoff, groundwater storage, and sediment and nutrient transport within watershed areas. Ecosystem components such as wetlands, which can contribute to the reduction of water pollution and the enhancement of groundwater recharge, are altered by LULC modifications. This study evaluates how wetlands in the Big Sunflower River Watershed (BSRW) have changed in recent years and quantified their impacts on streamflow, water quality, and groundwater storage using the Soil and Water Assessment Tool (SWAT). The model was well calibrated and validated prior to its application. Our study showed that the maximum increase in wetland areas within the sub-watersheds of interest was 26% from 2008 to 2020. The maximum changes in reduction due to the increase in wetland areas were determined by 2% for streamflow, 37% for total suspended solids, 13% for total phosphorus (TP), 4% for total nitrogen (TN), and the maximum increase in shallow groundwater storage by 90 mm from 2008 to 2020 only in the selected sub-basins. However, the central part of the watershed experienced average declines of groundwater levels up to 176 mm per year due to water withdrawal for irrigation or other uses. This study also found that restoration of 460 to 550 ha of wetlands could increase the reduction of discharge by 20%, sediment by 25%, TN by 18%, and TP by 12%. This study highlights the importance of wetland conservation for water quality improvement and management of groundwater resources.

Keywords: LULC; groundwater; hydrology; SWAT; sediments; nutrients

Citation: Nepal, D.; Parajuli, P.; Ouyang, Y.; To, F.; Wijewardane, N.; Venishetty, V. Evaluation of Wetland Area Effects on Hydrology and Water Quality at Watershed Scale. *Resources* **2024**, *13*, 114. https://doi.org/10.3390/resources13080114

Academic Editor: Diego Copetti

Received: 24 June 2024
Revised: 14 August 2024
Accepted: 19 August 2024
Published: 22 August 2024

1. Introduction

Land use and land cover (LULC) alterations are driving forces for unprecedented changes in environmental systems at local, regional, and global scales, leading to the expansion of urban areas, deforestation, and deterioration of soil and water quality [1]. The potential effects of LULC changes on wetland ecosystems are of special interest since these ecosystems are known to be vulnerable to anthropogenic and human-induced perturbations [2]. Previous research has confirmed that LULC vicissitudes can result in wetland area modification due to human activities such as the expansion of agriculture and urban areas [3,4]. Wetlands are among the most diverse ecosystems providing important ecological services to mankind [3], so it is imperative to study the effects of LULC changes on wetland dynamics.

Wetlands are the intermediate lands between terrestrial and deep-water ecosystems where the land is covered by shallow water, either seasonally or permanently [5]. They are distinct ecosystems with critical hydrological roles [6] such as providing flood-storage benefits [7], increasing groundwater recharge [8], and entrapping sediments and nutrients [9]. The LULC modifications may alter wetland areas, potentially affecting their functional characteristics [10] and increasing water pollution. Anthropogenic perturbations affect the water quality and hydrological components such as runoff, infiltration, evapotranspiration,

flood frequency, sediment, and nutrient concentrations within a watershed area [11–14]. In particular, agricultural operations such as tillage, and the application of chemicals and fertilizers are considered as significant sources of non-point source (NPS) pollutants. The expansion of agricultural areas may exacerbate water quality deterioration due to the increased discharge of NPS pollutants to nearby water bodies [11]. In this context, wetlands play a vital role in trapping pollutants and maintaining water quality in the surrounding environment. Understanding the impact of LULC changes on wetland areas facilitates the better management of these resources to ensure their continued ecological benefits in terms of retaining flow, pollution, and recharging groundwater

The Mississippi River Alluvial Valley (MRAV; 89° to 92° W longitude and 29° to 37° N latitude), where the Big Sunflower River Watershed (BSRW) lies, lost around 25% of its wetlands from 1930 to 2010 due to LULC changes [15]. Historically, 75% of more than 10 million ha of forested wetlands in the MRAV has been lost because of agricultural expansion and flood control project implementations [16]. The BSRW within MRAV is an agriculture-intensive watershed, where sediment and nutrient loads are generated from agricultural management operations such as conventional tillage, crop rotation, fertilizer, and pesticide applications [17]. In addition, irrigation in agricultural areas extensively uses groundwater resources, causing depletion of groundwater levels [18]. The wetlands present in the watershed area serve as natural sinks by retaining water quality pollutants, as well as recharging groundwater. Previous research demonstrated that 90% of nitrogen and phosphorus were reduced by forested wetlands within a site in the Mississippi Delta that had been exposed to wastewater effluent [19]. The wetlands in the Mississippi Delta within the Yazoo River Basin have helped to sustain water quality by trapping suspended sediment, nutrients, and pesticides contributed by agricultural runoff [20]. Similarly, the wetlands in the Mississippi Delta have also contributed to aquifer recharge, thus increasing groundwater storage [21].

In Mississippi, some of the wetland areas have been restored due to the continued fallowness of marginal agricultural lands and a decline in the rate of loss of forested areas resulting from a decline in the agricultural economy and a rise in recreational values [20]. Additionally, several private and government agencies participate in wetland conservation and restoration activities [20]. Some of the important activities include the 1972 Clean Water Act, the 1986 Emergency Wetlands Resources Act, the 1990 Food, Agriculture, Conservation, and Trade Act, as well as wetland conservation standards and regulations formulated by the Mississippi Department of Wildlife, Fisheries, and Parks, and the Mississippi Department of Environmental Quality. These factors make it plausible that certain wetland regions have been restored in recent years. This prompts the need for research focused on investigating how wetlands have changed recently in Mississippi watersheds and the quantification of their impacts on hydrology and water quality. In this study, wetland areal changes over a 12-year period (2008–2020) were evaluated, and their effects on surface water quality, quantity, and groundwater storage were assessed. The choice of this period is based on the availability of wetland data from the LULC classification. The wetland information was extracted from the cropland data layer provided by National Agricultural Statistics Service which included the wetland classification from 2008.

Hydrological models have been developed to evaluate hydrological processes. Several hydrological models have been applied to assess wetland hydrology and water quality, such as the Wetlands Dynamic Water Budget Model [22], HEC-1 [23,24], SWAMP-MOD [25], FLATWOODS [26], and SWAT [27]. SWAT was applied in research conducted by Bekele et al. [28] to analyze the impacts of constructed wetlands on hydrology and water quality in two agriculture-dominated Illinois watersheds. Additionally, because of its ability to simulate NPS pollutants and agricultural management operations, SWAT has been used widely for wetland hydrologic and water quality simulations in agricultural watersheds [29–31]. This study being conducted in an agricultural watershed to quantify the hydrological and water quality benefits of wetlands, SWAT was preferred due to its

comprehensive capacity to simulate the agricultural operations, NPS pollution dynamics, groundwater storage, and their interaction with wetland processes.

Several studies have documented the impacts of LULC alterations on surface water quality and quantity in different watersheds [32–34], including BSRW [35]. However, a research gap exists, particularly in BSRW in relation to the temporal changes of wetlands and their associated effects on the surface water quality and quantity, and groundwater storage. The present study attempts to fill the identified research gap and is the first of its kind in BSRW, which is characterized by declining aquifers, high levels of NPS pollution, and impaired water quality [17]. The evaluation of temporal changes in wetlands facilitates the understanding of how wetlands have contributed to pollution mitigation and groundwater recharge over time. The specific objectives of this research were to: (a) develop a calibrated and validated SWAT model against flow, total suspended solids (TSS), total phosphorus (TP), total nitrogen (TN), and groundwater level changes, and (b) evaluate the trend of wetland area changes and their effects on surface water quality, quantity, and shallow groundwater storage.

2. Materials and Methods

2.1. Watershed Description

The BSRW is in the Mississippi Alluvial Plain within the Mississippi Delta. The model-estimated drainage area of the watershed is 8326 km^2 and lies within 11 counties in northwestern Mississippi. The elevation of the watershed ranges from 23 to 71 m above mean sea level. The BSRW is an agriculturally dominated watershed with soybean, corn, rice, and cotton as major crop types according to land cover classification provided by the National Agricultural Statistics Service [36] (Figure 1). The major types of soil in the area are Alligator, Dowling, Dundee, Forestdale, and Sharkey, according to soil data provided by the National Resources Conservation Service [37], all of which have high silt and clay percentages contributing to higher surface runoff and low permeability. Due to such soil characteristics, only a small amount of surface water infiltrates through the soil profile into the Mississippi River Valley Alluvial Aquifer (MRVAA) [38]. Moreover, the majority of water utilized for agriculture and industry in the Mississippi Delta comes from the MRVAA through pumping, causing groundwater depletion [38].

2.2. SWAT Model Description

SWAT is a process-based semi-distributed watershed modeling tool that requires a variety of spatial and temporal data on the physical characteristics of a watershed, such as surface elevation, land use, soil type, climate data, and management data, and predicts the impacts of land-use change, climate change, and management decisions on surface and groundwater [27,39]. SWAT delineates watersheds into subbasins which are further divided into smaller areas based on unique land use, soil, and slope attributes known as hydrologic response units (HRUs). Each HRU can be modified by the user to incorporate certain management decisions, as well as parameters that control the movement of surface water, groundwater, and pollutants [40]. The hydrological cycle simulated by the modeling tool is based on the water balance calculated at the HRU level and is controlled by climatic factors such as precipitation, temperature, solar radiation, relative humidity, and wind speed [40]. In this study, the Digital Elevation Model (DEM), soil data, and LULC data, each with a spatial resolution of 30 m, were provided to the model along with weather data, management operations, and wetland parameters to determine surface runoff, shallow groundwater storage, and water quality outputs (Figure 2).

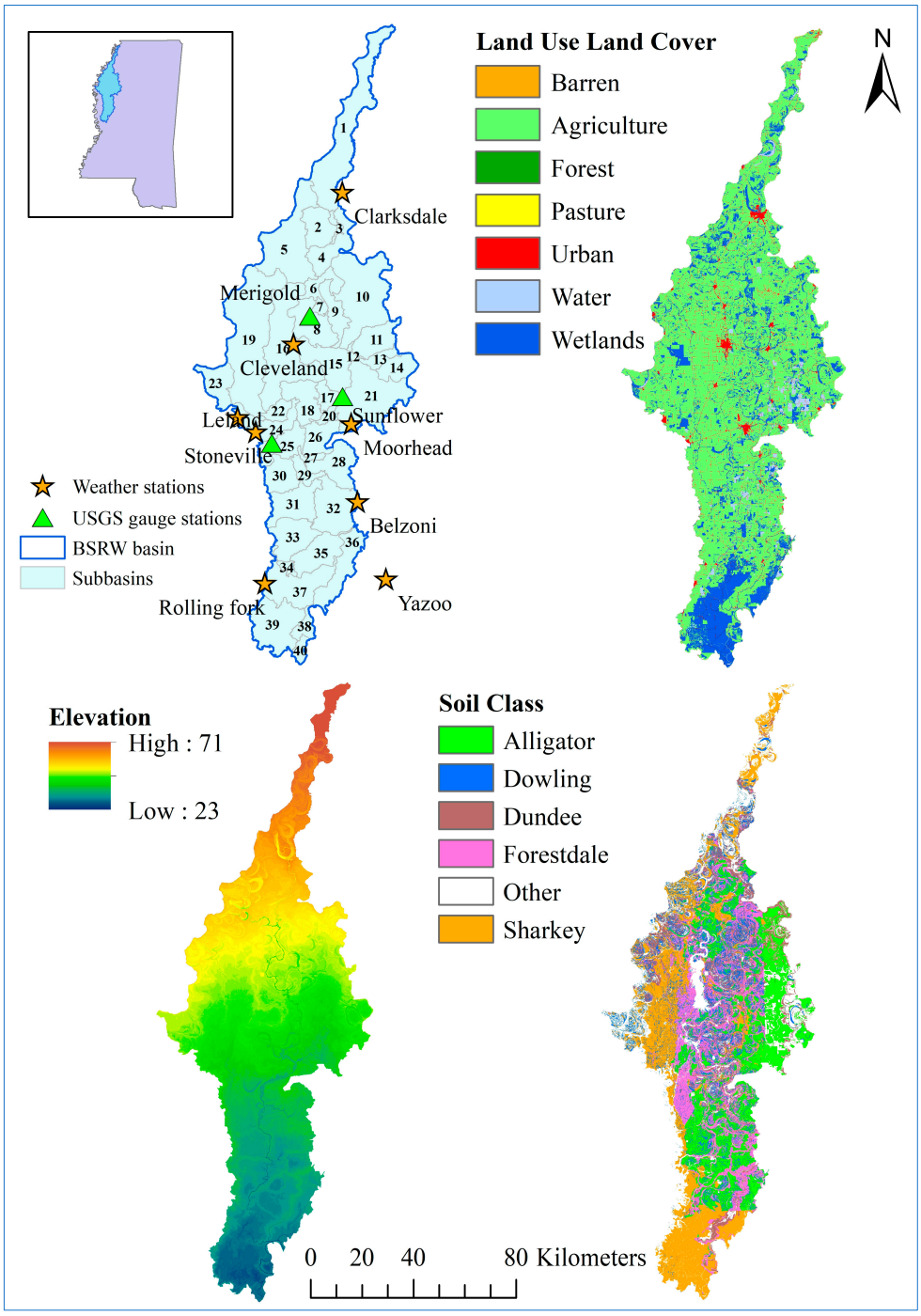

Figure 1. Location map of the Big Sunflower River Watershed showing locations of weather stations, land use, land cover, elevation, and soil classification.

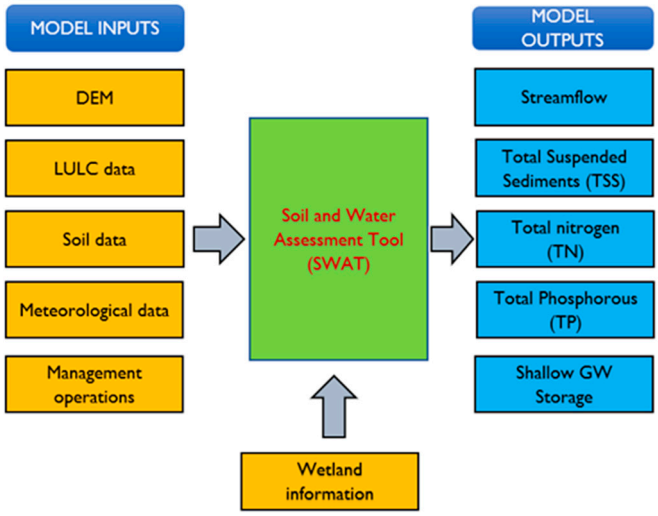

Figure 2. General steps used in the SWAT modeling process for wetland simulation.

SWAT simulates shallow and deep aquifers in each subbasin [41]. Processes such as infiltration, seepage, and percolation contribute to groundwater recharge. The shallow aquifer is unconfined and contributes to percolation to the deep aquifer or base flow within the watershed, whereas a deep aquifer is confined and contributes to base flow outside the watershed. Water from shallow groundwater storage can move upwards to the overlying unsaturated zone by evaporation from the capillary fringe (a saturated zone above the groundwater table) or by plant uptake. The model also allows water to be removed from shallow aquifers if the shallow aquifer is designated as the irrigation source. To assign a shallow aquifer as the irrigation source, SWAT requires information on the subbasin number, in which the shallow aquifer is located (IRRNO), and the irrigation code (IRRSC). IRRSC informs the model about the type of water body from which irrigation water is being diverted [41]. The water balance in the shallow aquifer is calculated using Equation (1) [40]:

$$aq_{sh,i} = aq_{sh,i-1} + w_{recharge,sh} - Q_{gw} - w_{revap} - w_{pump,sh} \quad (1)$$

Here, $aq_{sh,i}$ is the stored water in the shallow aquifer on day i (mm), aqsh,i-1 is the stored water in the shallow aquifer on day i-1 (mm), $w_{recharge,sh}$ is the shallow aquifer recharge on day i (mm), Q_{gw} is the base flow contributed to the main channel on day i (mm), w_{revap} is the amount of water that enters the overlying soil zone as a result of water shortages on day i (mm), $w_{pump,sh}$ is the water removed by pumping from the shallow aquifer on day i (mm).

The SWAT model has been applied successfully to simulate streamflow, sediment yield, nutrient yield, and groundwater storage at a watershed scale [42–44]. SWAT estimates streamflow using the Soil Conservation Service (SCS) curve number procedure, and sediment yield using the Modified Universal Soil Loss Equation (MUSLE) [45]. The plants' use of nutrients such as nitrogen and phosphorous are estimated using the supply and demand approach. Organic nitrogen and phosphorous are removed from the soil through the mass flow of water. Similarly, sediment transport of nitrogen and phosphorous are estimated using a loading function as described in Neitsch et al. [40].

In the current investigation, three historical LULC data layers from 2008, 2014, and 2020 were applied individually to three separate SWAT models with other inputs being the same to evaluate the effects of wetland areal changes on streamflow, sediment yield, nutrient yield, and groundwater storage over a period of 12 years. The change in the LULC data layer had no significant impact on the calibration and validation statistics, and the statistics remained within acceptable limits suggested by Gassman et al. [46]. The analysis of wetland areal changes was conducted between 2008 and 2020, and three LULC data layers from 2008, 2014, and 2020 were utilized to capture the underlying trend.

2.3. SWAT Model Inputs

The watershed was divided into 40 subbasins and 564 HRUs. For the HRU definition, this study used a threshold of 10% for land use, soil, and slope classes. A threshold provides a criterion to exclude minor land use, slope, and soil classes. Following the elimination process, the areas of the remaining land use, soil, and slope classes were reapportioned so that 100% of the land use, soil, and slope areas were modeled. This approach ensured that the dominant land use, soil, and slope classes were accurately reflected, while eliminating insignificant classes [47]. The SWAT model inputs used in the present investigation included the following: A 30 m × 30 m DEM from the United States Geological Survey (USGS) website [48], land use data layers in the form of Cropland Data Layer (CDL) obtained from the United States Department of Agriculture (USDA), National Agricultural Statistics Service (NASS) [36], soil data from the National Resources Conservation Service (NRCS), Soil Survey Geographic Database (SSURGO) [37], meteorological data including daily precipitation and temperature from the National Oceanic and Atmospheric Administration (NOAA) [49] for 8 weather stations, as shown in Figure 1, additional weather data on relative humidity, solar radiation, and wind speed from the Global weather data for SWAT [50], management operations such as schedules and amounts of irrigation water, fertilizers, pesticides, planting, and harvesting dates, and tillage dates for four major crops—soybean, cotton, corn, and rice—from the Mississippi Agricultural and Forestry Experiment Station (MAFES) variety trials' annual reports [51]. The shallow aquifer was assigned as the source of irrigation in each subbasin by incorporating the information related to irrigation source location and irrigation code on the SWAT management input table [41] All agricultural lands were irrigated through groundwater since groundwater serves as the main source for irrigation in BSRW [52].

2.4. Model Calibration and Validation Procedures

To assess the model performance in simulating streamflow, TSS, TP, TN, and multisite SWAT calibration and validation were conducted at the outlets of subbasins 7 (Merigold, USGS gauge: 07288280), 15 (Sunflower, USGS gauge: 07288500), and 24 (Leland, USGS gauge: 07288650), as shown in Figure 1. Monthly calibration of streamflow was performed from January 2008 to December 2012, and validation from January 2013 to December 2017 using observed discharge data obtained from the three USGS gauge stations. The observed TSS, TP, and TN concentration data were available at an interval of every 15 days from 2016 to 2018. Therefore, to convert the data into continuous loads, the Load Estimator (LOADEST) [53] regression tool was used. Continuous water quality data aggregated to monthly loads were used for model calibration (January 2016–June 2017) and validation (July 2017–October 2018) at three USGS gauge stations. The LOADEST regression model has been successfully used in hydrological modeling studies to estimate time series of water quality data [17,54,55]. The LOADEST model performed well in estimating the TSS, TP, and TN loads at all three-gauge stations with the coefficient of determination (R^2) [56] and Nash–Sutcliffe Efficiency (NSE) [57] for the regression models greater than 0.86 and 0.50, respectively.

For calibration and validation purposes, an auto-calibration algorithm Sequential Uncertainty Fitting (SUFI-2) within SWAT Calibration and Uncertainty Procedures (SWAT-CUP) [58] was used. In SUFI-2, two statistics, namely P-factor and R-factor, are calculated to predict model uncertainty. P-factor is the percentage of observations captured by the 95% prediction uncertainty (95PPU), calculated using Latin hypercube sampling at 2.5% and 97.5% levels, and R-factor is the average width of the 95PPU divided by the standard deviation of the measured data [58]. A P-factor of 1 and an R-factor of 0 indicate a perfect fit between the measured and simulated data. The sensitivity analysis was performed using T-statistic and *p*-value to provide an understanding of the parameters that had the largest impact on the simulated flow, TSS, TP, and TN. The T-statistic gives the measure of sensitivity, and the *p*-value provides the measure of the significance of a parameter. A low *p*-value (<0.05) and a high T-statistic suggests that the parameter has some effect on the

response variable [58]. In each iteration, SUFI-2 was simulated 1500 times to get the final values of the parameters.

The calibration procedure involved altering 14 streamflow-related parameters, 12 sediment-related parameters, 8 phosphorous-related parameters, and 6 nitrogen-related parameters to optimize the objective function, NSE in SWAT-CUP. In addition to NSE, R^2 was used to analyze the model performance. The values of NSE and R^2 ranged from $-\infty$ to 1, and from 0 to 1, respectively. The higher the values of these model performance indicators, the better the model prediction, with 1 being perfect. Table 1 summarizes the parameter description [39], their ranges, and fitted values for streamflow, TSS, TP, and TN. To assess the effects of wetlands on groundwater, calibration and validation were conducted for groundwater table depth changes. The groundwater table depth data provided by Yazoo Mississippi Delta Joint Water Management District (YMD) were available only twice a year, in spring (mostly April) and in fall (mostly October). Therefore, calibration and validation were performed on a seasonal scale. This means that the changes in observed water table depths between spring and fall were compared to the changes in simulated water table depths between spring and fall from the years 2008 to 2020. Two areas were chosen within the watershed for spatial calibration (subbasins 8 and 15) and validation (subbasins 31 and 33) (Figure 3). These areas were selected based on the lower spatial variance in water-table depths and continuous data availability from 2008 to 2020. Altogether, 41 monitoring wells were selected, 22 at calibration subbasins and 19 at validation subbasins. The observed and simulated values were spatially averaged for each season, and a spatial calibration and validation approach was applied in these areas. The changes in groundwater table depths cannot be obtained in SWAT, however, the changes in shallow aquifer storage (SA_ST) can be derived, which is an HRU-level output. This parameter gives the cumulative net result considering all the inputs and outputs during a certain time interval. To acquire an approximate groundwater elevation change caused by a change in shallow aquifer storage, a ratio of its change to specific yield can be computed [42]. The specific yield for the shallow aquifer is equivalent to porosity and is defined as the ratio of the volume of water draining by gravity to the total volume of aquifer materials [39]. The solver tool in Microsoft Excel was utilized to calculate the specific yield by maximizing the objective function, NSE. In addition to NSE, R^2 was also calculated to evaluate the accuracy of the output.

Table 1. Flow and water quality-related model parameters used for SWAT-CUP model calibration and validation.

Variable	Parameter Name	Description	Fitted Value	Min. Value	Max. Value
Streamflow	r___CN2.mgt [a]	SCS curve number	−0.09	−0.15	0.02
	v__ESCO.hru [b]	Soil evaporation compensation factor	0.41	0.13	0.80
	v__CH_N2.rte	Manning's roughness for the main channel	0.004	0.004	0.01
	v__OV_N.hru	Manning's roughness for overland flow	0.35	0.20	0.36
	v__SURLAG.bsn	Surface runoff lag coefficient	5.96	4.00	9.50
	r__SOL_K.sol	Saturated hydraulic conductivity of soil layers (mm/h)	−0.24	−0.24	0.27
	v__ALPHA_BF.gw	Baseflow alpha factor (1/days)	0.73	0.44	0.81
	v__GW_DELAY.gw	Groundwater delay (days)	299.74	100.22	300.08
	v__GW_REVAP.gw	Coefficient of groundwater "revap"	0.11	0.00	0.13
	v__SFTMP.bsn	Snowfall temperature (°C)	−4.61	−5.00	0.77
	r__SLSOIL.hru	Slope length for lateral subsurface flow (m)	0.45	0.18	0.50
	r__SLSUBBSN.hru	Average slope length (m)	0.03	−0.20	0.09
	v__GWQMN.gw	Threshold water depth in shallow aquifer to trigger return flow (mm)	867.78	795.84	3598.66
	r__SOL_AWC.sol	Available water capacity of soil layer (mm/mm)	−0.50	−0.50	0.07

Table 1. *Cont.*

Variable	Parameter Name	Description	Fitted Value	Min. Value	Max. Value
TSS	v__USLE_P.mgt	Universal Soil Loss Equation (USLE) support practice factor	0.76	0.59	0.77
	r__USLE_K.sol	USLE soil erodibility factor	−0.51	−0.51	−0.44
	r__HRU_SLP.hru	Average slope steepness (m/m)	0.27	0.27	0.40
	v__CH_ERODMO.rte	Monthly channel erodibility factor	0.03	0.00	0.08
	r__USLE_C.plant.dat	USLE crop cover factor	−0.18	−0.20	−0.13
	v__PRF_BSN.bsn	Main channel peak rate adjustment factor for sediment routing	0.14	0.08	0.16
	v__SPEXP.bsn	Exponent parameter to calculate sediment re-entrained in channel sediment routing	1.08	1.01	1.14
	v__CH_COV1.rte	Channel erodibility factor	0.00	−0.01	0.06
	v__CH_COV2.rte	Channel cover factor	0.16	0.14	0.17
	v__SPCON.bsn	Linear parameter to calculate sediment re-entrained during channel sediment routing	0.00	0.00	0.00
	v__ADJ_PKR.bsn	Peak rate adjustment factor for sediment routing in tributary channels	1.59	1.47	1.62
	v__LAT_SED.hru	Lateral and groundwater flow sediment concentration (mg/L)	1408.48	1355.95	1451.99
TP	v__PHOSKD.bsn	Coefficient of phosphorus soil partitioning (m^3/Mg)	120.48	94.08	125.65
	v__PPERCO.bsn	Coefficient of phosphorous percolation (10 m^3/Mg)	10.67	10.19	11.21
	v__BC4.swq	Rate constant for mineralization of organic phosphorus to dissolved phosphorus (day^{-1})	0.14	0.02	0.17
	v__RS2.swq	Benthic source rate for dissolved phosphorus (P) (mgP/(m^2 day))	0.03	0.02	0.06
	v__RS5.swq	Settling rate of organic phosphorus (day^{-1})	0.02	0.01	0.04
	v__PSP.bsn	Phosphorus availability index	0.35	0.29	0.55
	v__P_UPDIS.bsn	Phosphorus uptake distribution	20.52	20.37	61.12
	v__ERORGP.hru	Phosphorus enrichment ratio for loading with sediment	0.41	0.10	2.91
TN	v__SHALLST_N.gw	Initial nitrate concentration in shallow aquifer (mgN/L)	571.12	421.99	807.34
	v__RCN.bsn	Nitrogen concentration in rainfall (mgN/L)	6.60	4.92	9.80
	v__NPERCO.bsn	Nitrate percolation coefficient	0.06	0.00	0.15
	v__CMN.bsn	Humus mineralization rate factor of active nutrients	0.0014	0.0013	0.002
	v__SOL_NO3().chm	Initial concentration of NO_3 in soil layer (ppm)	5.86	0.00	45.65
	v__FRT_SURFACE.mgt	Fertilizer fraction applied to top 10 mm of soil	0.92	0.75	1.00

[a] r__ denotes original value was multiplied by (1 + fitted value); [b] v__ denotes original value was replaced by the fitted value.

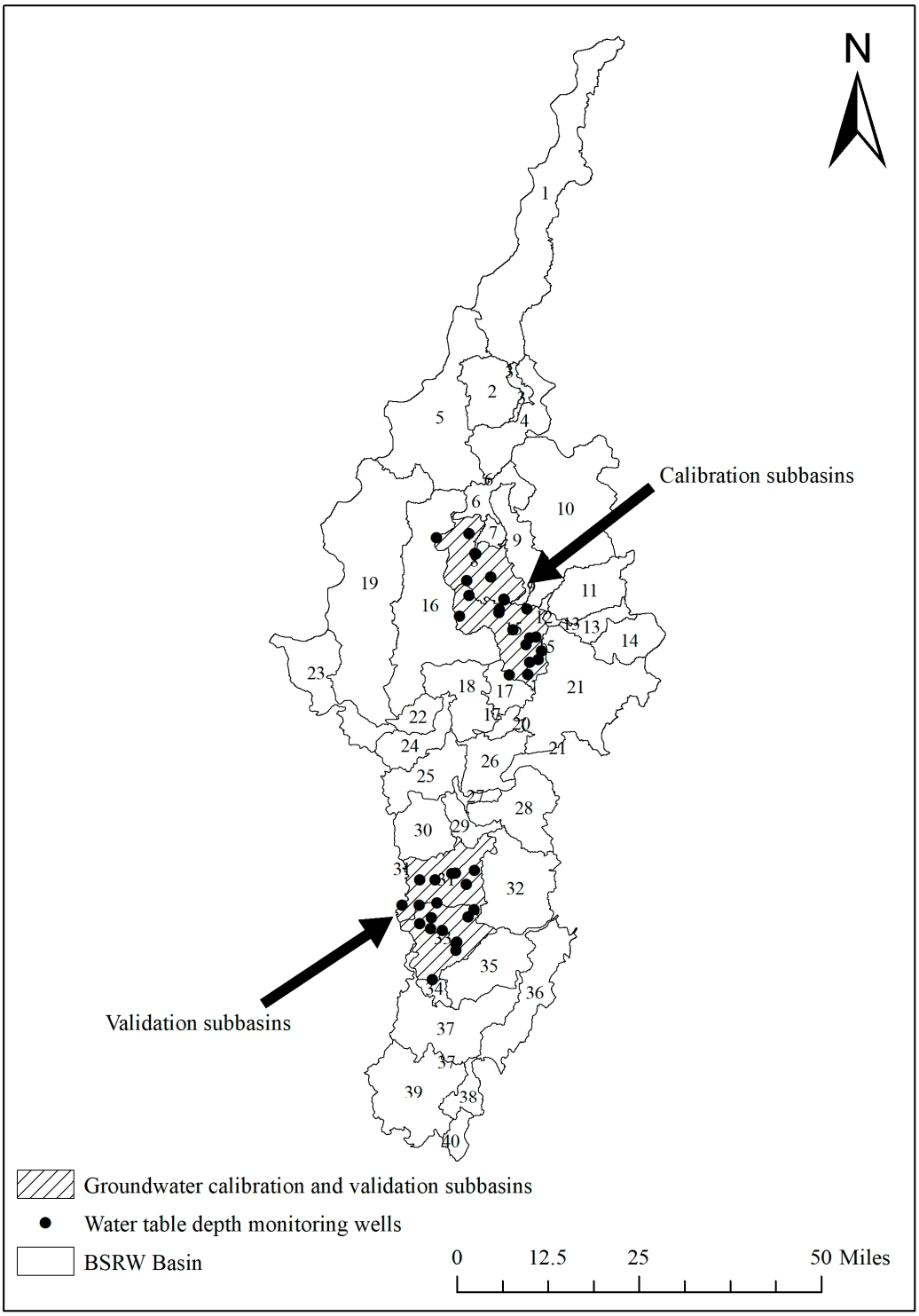

Figure 3. Watershed map showing groundwater monitoring wells, model calibration, and validation subbasins.

2.5. Wetland Scenario

To investigate the historical trend of wetland changes within the BSRW over the past 12 years from 2008 to 2020, land cover data from 2008, 2014, and 2020 provided by USDA, NASS, were utilized. Wetland surface areas were extracted from both the forested and non-forested wetland classes within CDL. The data layers were applied to three separate SWAT models, along with the wetland information. To ascertain the effects of wetlands on streamflow, sediments, nutrients, and shallow groundwater storage, results from two

separate models—one before wetland simulation and one after wetland simulation—were differentiated for each case (i.e., 2008, 2014, and 2020). These effects were calculated as percentage reduction on flow and water quality parameters based on Equation (2).

$$\text{Reduction } (\%) = \frac{\text{variables before wetland simulation} - \text{variables after wetland simulation}}{\text{variables before wetland simulation}} \times 100 \quad (2)$$

The SWAT model allowed a single wetland in each subbasin, applied by aggregating all wetland areas within the subbasins. The principal area of the wetland was obtained from the CDL data layer. The principal volume was calculated as the principal area multiplied by the average wetland depth. A range of water depth values from 0.2 m to 1 m was used based on previous studies as shown in Table 2 and the principal volume parameter was calibrated, resulting in an optimal average depth of 0.9 m. To estimate maximum surface area and maximum volume, a range of multiples of the principal area (2–3×) and principal volume (3–5×) were chosen and calibrated. This resulted in the optimal multiples of 2.5 and 4, respectively. It was assumed that the wetlands were in operation at the beginning of the simulation. A 3-year warm-up period was applied in SWAT, which allowed the model to achieve the water processes simulation properly, and the output was obtained from the fourth year. Hence, the initial volume of water and initial sediment concentration in wetlands were set to 0. The equilibrium sediment concentration in wetlands was calibrated. Hydraulic conductivity through the wetland bottom was measured to be 0.15 mm/h from calibration. According to [39], the phosphorus settling rates mostly fall in the range of 5 to 20 m/year for natural lakes. Phosphorus and nitrogen settling rates were calibrated within this range. An insight into the parameter ranges was obtained from the previous literature, as shown in Table 2.

Table 2. Parameters used for wetland simulation in SWAT.

Wetland Parameters	Parameter Values in Previous Studies	References	Calibrated/Used Values
Depth of wetland	0.2 m 0.6 m and 0.67 m 0.85 m 1 m	[59] [60] [61] [62]	0.9 m
Maximum surface area			6643 ha (subbasin 15); 4866 ha (subbasin 33)
Maximum volume			9566 ha-m (subbasin 15); 7007 ha-m (subbasin 33)
Initial water volume	0	[63]	0
Initial sediment concentration			0
Equilibrium sediment concentration			200 mg/L
Hydraulic conductivity	0.2 mm/h for reservoir simulation	[64]	0.15 mm/h
P and N settling rate	5 to 20 m/year	[39]	12 m/year and 11 m/year

To evaluate the effects of wetlands, subbasins 15 and 33 were taken into account. The decision to concentrate the investigation on these subbasins was due to reasonable model performances in simulating flow, sediment, nutrients, and seasonal groundwater level changes within these subbasins, ensuring a more realistic representation of the hydrological processes. Moreover, subbasin 15 was of particular interest since it lies within the "cone of depression" where the largest decline in the water table was observed due to groundwater pumping for irrigation [65]. We were also interested in assessing the effects of wetlands in a subbasin that is predominantly agricultural since agriculture is the primary source of water quality pollution in the BSRW. About 86% of the area in subbasin 33 was used for agriculture in 2020.

Total areas of wetlands in subbasins 15 and 33, based on the land cover data layer provided by USDA, NASS for the years 2008, 2014, and 2020, are shown in Table 3. Figure 4 shows the percentage of wetlands in each subbasin. The overall wetland area in subbasin 33 is less than that in subbasin 15 because of the larger agricultural area percentage in

subbasin 33. Between the years 2008 and 2020, the total areas of wetlands in the subbasins under consideration experienced an increasing trend, which can affect hydrology and water quality. In subbasin 15, the total wetland area increased from about 9% of the subbasin area to 11% of the subbasin area. Similarly, in subbasin 33, the total wetland area increased from about 7% of the subbasin area to 9% of the subbasin area. While the wetlands increased in these subbasins, the agricultural land cover was found to decrease. For instance, in subbasin 33, the agricultural land cover was around 88% in 2008, which reduced to 86% in 2020.

Table 3. Wetland areas in subbasin 15 and subbasin 33 in 2008, 2014, and 2020.

Sub-Watersheds	Sub-Watershed Area (km^2)	Wetland Areas (km^2)		
		Year 2008	Year 2014	Year 2020
15	245.24	23.08	25.75	26.57
33	214.39	15.40	17.97	19.46

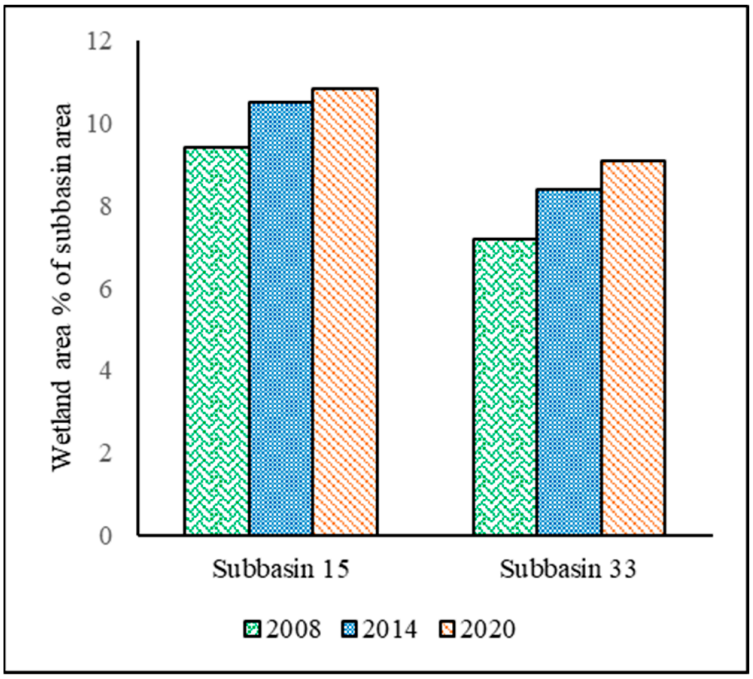

Figure 4. Percentage of wetlands in watershed sub-basins 15 and 33 in the years 2008, 2014, and 2020.

3. Results

3.1. Streamflow Calibration and Validation

Among all the selected parameters, CN2, ESCO, OV_N, CH_N2, SURLAG, and SOL_K were found to be the most sensitive with a *p*-value less than 0.05. These parameters determine the soil water conditions, evaporation, permeability, land use conditions, as well as the rate and amount of runoff which influence the streamflow directly.

The model was calibrated and validated for monthly streamflow with reasonable accuracies, where R^2 ranged from 0.60 to 0.87, and NSE ranged from 0.60 to 0.84. Table 4 shows the summary of statistics obtained during the calibration and validation of streamflow at three USGS gauge stations. The time series of simulated and measured streamflow data during calibration and validation at the Sunflower gauge station are presented in Figure 5.

Table 4. Model performance during calibration and validation of streamflow at 3 USGS gauge stations.

Station	Calibration				Validation			
	P-Factor	R-Factor	R^2	NSE	P-Factor	R-Factor	R^2	NSE
Merigold	0.87	0.86	0.72	0.70	0.79	0.84	0.60	0.60
Sunflower	0.78	0.74	0.76	0.76	0.85	0.84	0.87	0.84
Leland	0.68	0.80	0.70	0.64	0.76	1.26	0.82	0.79

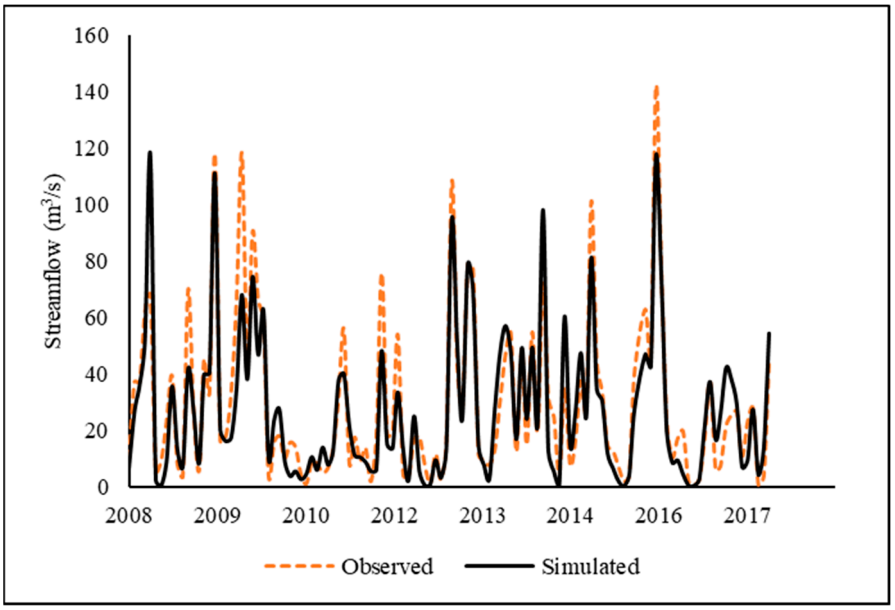

Figure 5. Simulated and measured streamflow during calibration and validation at Sunflower gauge station.

3.2. Total Suspended Solids Calibration and Validation

Among all the selected parameters, USLE_P, USLE_K, HRU_SLP, CH_ERODMO, USLE_C, PRF_BSN, and SPEXP were found to be the most sensitive parameters with *p*-values less than 0.05. These parameters are associated with features such as land cover, soil erodibility, slope, channel degradation, and sediment re-entrainment which affect the rate and amount of sediment directly.

The model was calibrated and validated for monthly TSS with acceptable accuracies, where R^2 ranged from 0.68 to 0.94, and NSE ranged from 0.48 to 0.85. Table 5 shows the summary of statistics obtained during the calibration and validation of TSS at three USGS gauge stations. The time series of simulated and observed TSS data during calibration and validation at the Sunflower gauge station are presented in Figure 6. Despite the reasonable statistics, there was a difference between observed and simulated TSS loads in February 2018 due to SWAT's limitation in capturing peak flow and floodplain erosion [66,67]. Additionally, the TSS loads are highly affected by factors such as tillage, especially in agricultural watersheds like BSRW. The rate, time, and space of such operations are variable, thus creating uncertainty in capturing peak TSS loads.

Table 5. Model performance during calibration and validation of TSS at 3 USGS gauge stations.

Station	Calibration				Validation			
	P-Factor	R-Factor	R^2	NSE	P-Factor	R-Factor	R^2	NSE
Merigold	0.83	0.67	0.80	0.72	0.72	1.10	0.68	0.62
Sunflower	0.83	0.76	0.88	0.85	0.56	0.37	0.77	0.48
Leland	0.78	0.75	0.83	0.82	0.61	1.98	0.94	0.56

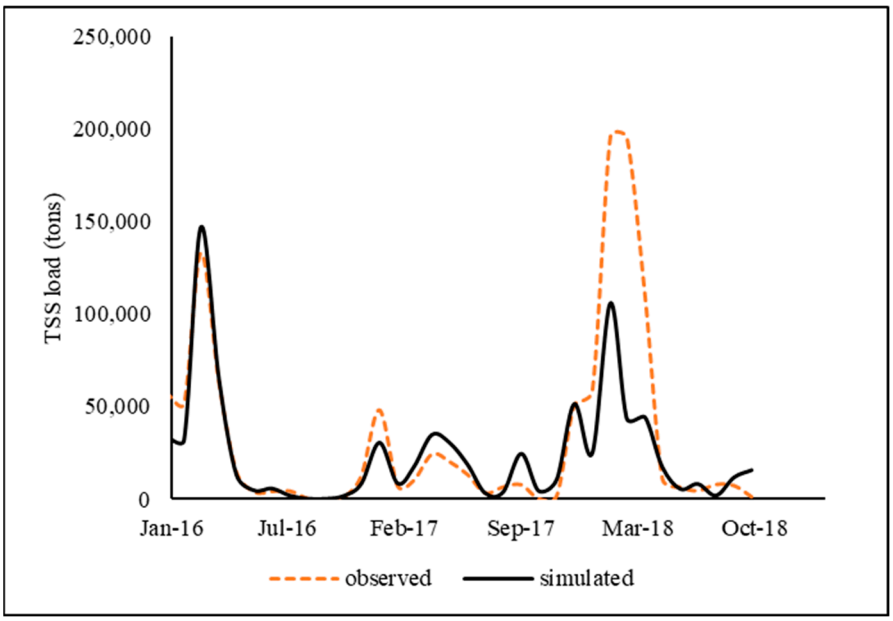

Figure 6. Simulated and measured TSS loads during calibration and validation at Sunflower gauge station.

3.3. Total Phosphorus Calibration and Validation

Among all the selected parameters, ERORGP, P_UPDIS, PHOSKD, RS5, and PPERCO were found to be the most sensitive parameters, with *p*-values less than 0.05. These parameters dictate phosphorous transport, uptake by plants, settling, and percolation. The model was calibrated and validated for monthly TP with acceptable accuracies, where R^2 ranged from 0.40 to 0.95, and NSE ranged from 0.05 to 0.84. Table 6 summarizes the statistics obtained during the calibration and validation of TP at three USGS gauge stations. The time series of observed and simulated TP loads during calibration and validation at the Sunflower gauge station is shown in Figure 7.

Table 6. Model performance during calibration and validation of TP at 3 USGS gauge stations.

Station	Calibration				Validation			
	P-Factor	R-Factor	R^2	NSE	P-Factor	R-Factor	R^2	NSE
Merigold	0.89	1.35	0.50	0.40	0.56	0.25	0.50	0.05
Sunflower	0.94	2.11	0.86	0.84	0.44	0.25	0.81	0.30
Leland	0.94	1.95	0.40	0.23	0.50	0.29	0.95	0.53

3.4. Total Nitrogen Calibration and Validation

Among all the selected parameters, FRT_SURFACE and NPERCO were the most sensitive parameters, with *p*-values less than 0.05. These parameters control the fertilizer application to the soil surface, and nitrate removal in runoff from the surface, which directly influence the total nitrogen. The model was calibrated and validated for monthly TN with acceptable accuracies, where R2 ranged from 0.30 to 0.90, and NSE ranged from 0.04 to 0.84. Table 7 summarizes the statistics obtained during the calibration and validation of TN at three USGS gauge stations. The time series of observed and simulated TN loads during calibration and validation at the Sunflower gauge station is shown in Figure 8.

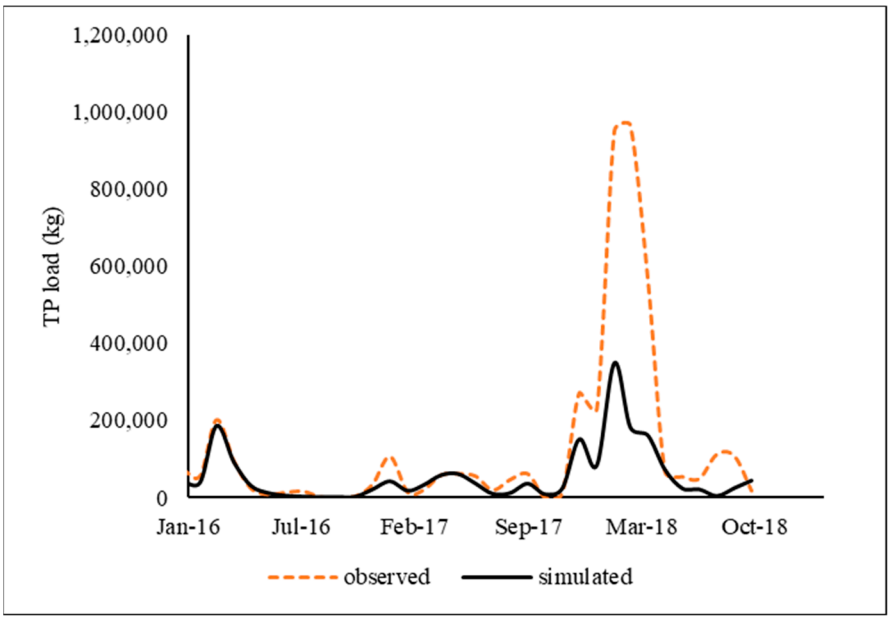

Figure 7. Simulated and measured TP loads during calibration and validation at Sunflower gauge station.

Table 7. Model performance during calibration and validation of TN at 3 USGS gauge stations.

Station	Calibration				Validation			
	P-Factor	R-Factor	R^2	NSE	P-Factor	R-Factor	R^2	NSE
Merigold	0.61	0.57	0.37	0.30	0.44	0.61	0.30	0.04
Sunflower	0.56	0.59	0.61	0.56	0.56	0.58	0.50	0.32
Leland	0.94	1.18	0.90	0.84	0.69	0.52	0.71	0.50

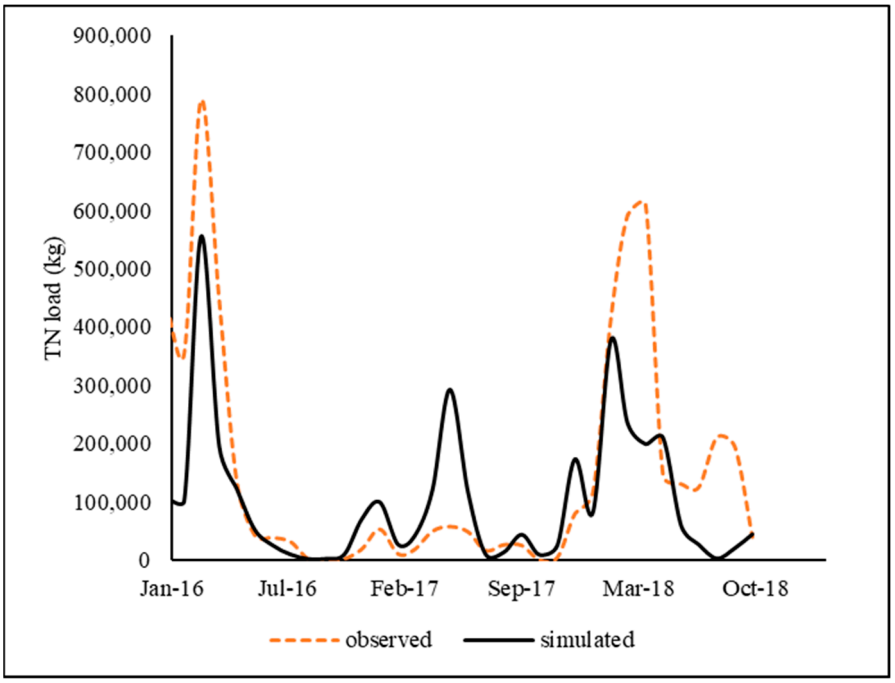

Figure 8. Simulated and measured TN loads during calibration and validation at Sunflower gauge station.

3.5. Groundwater Level Change Calibration and Validation

Spatial calibration and validation of seasonal groundwater level change were performed in subbasins 8 and 15, and in subbasins 31 and 33, respectively. The values of

R^2 were 0.34 and 0.52, and the values of NSE were 0.32 and 0.31 during calibration and validation, respectively. To maximize the statistical indicator, NSE, the solver tool estimated the optimal value of specific yield as 0.21. Figure 9 shows the observed and simulated groundwater level changes at the seasonal scale from 2008 to 2020 in the calibration and validation subbasins.

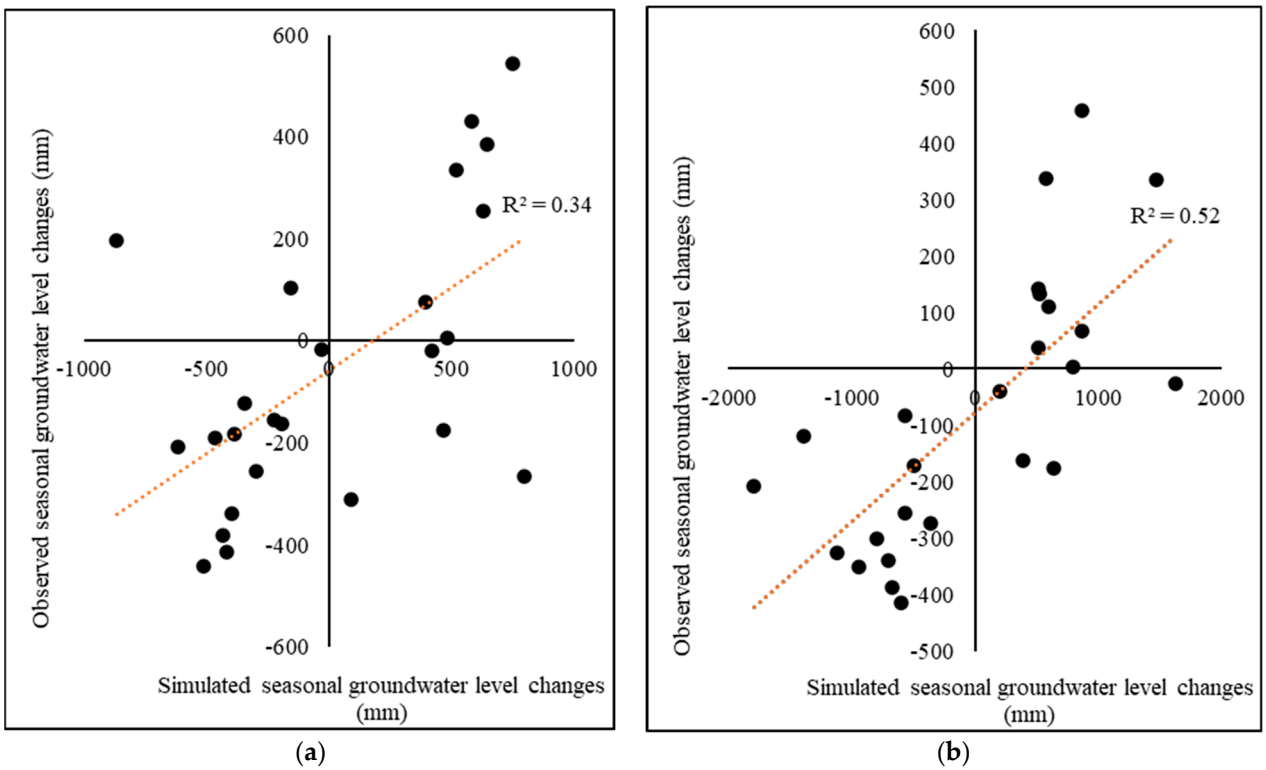

Figure 9. Simulated vs. observed seasonal groundwater level changes from 2008 to 2020 during model: (**a**) calibration, and (**b**) validation.

3.6. Effects of Wetlands on Flow and Water Quality

The increase in wetland areas from 2008 to 2020 led to an increment in the reduction of flow, sediments, and nutrients at the subbasin outlets. Flow reduction increased from about 9% to 11% from 2008 to 2020 in subbasin 15, and from about 1% to 2% in subbasin 33. Similarly, the sediment reduction increased from 86% to 89% in subbasin 15, and from 19% to 56% in subbasin 33. The discrepancy in TSS reduction between 2008 and 2020 was greater in subbasin 33 than in subbasin 15. This can be attributed to the fact that the percentage increase of wetland area between these years in subbasin 33 (26%) surpassed that of subbasin 15 (15%). The substantial difference in TSS reduction between 2014 and 2020 for subbasin 33 can be explained by the influence of precipitation. The average annual precipitation in subbasin 33 during 2020 exhibited a lower magnitude (1179 mm) compared to that of 2014 (1350 mm). The reduced inflow of water into the wetlands during the period of low precipitation resulted in decreased flow velocities, reducing the capacity of wetlands to transport sediment. Additionally, low precipitation reduced erosion in upstream regions, resulting in higher sediment retention within the wetlands. These factors account for a high TSS reduction during 2020, consequently leading to a significant difference between 2014 and 2020 (Table 8). The total phosphorous reduction in subbasin 15 increased from 31% to 44%, and from 8% to 13% in subbasin 33. Likewise, the total nitrogen reduction increased from 39% to 43% in subbasin 15 from 2008 to 2020, and from 10% to 13% in subbasin 33. Table 8 summarizes the increase in reduction percentages of streamflow, TSS, TN, and TP during the period from 2008 to 2020.

Table 8. Effects of wetlands on streamflow, TSS, TN, and TP reduction percentage.

Variables	Sub-Watershed	Reduction %			Reduction Increase% (2008–2014)	Reduction Increase% (2014–2020)	Reduction Increase% (2008–2020)
		Year 2008	Year 2014	Year 2020			
Streamflow	15	8.7	9.5	11	0.8	1.5	2.3
	33	1.5	1.7	2.1	0.2	0.4	0.6
TSS	15	86.1	87.2	89.1	1.1	1.9	3
	33	18.8	26.3	55.6	7.5	29.3	36.8
TN	15	39.5	42.0	42.7	2.5	0.7	3.2
	33	9.6	11.0	12.8	1.4	1.8	3.2
TP	15	31.3	40.0	44.1	8.7	4.1	12.8
	33	7.7	10.9	13.5	3.2	2.6	5.8

3.7. Effects of Wetlands on Shallow Groundwater Change

As a result of an increase in areas, the contribution to shallow groundwater storage by wetlands increased. In subbasin 15, the contribution to the shallow aquifer by wetlands was 40 mm higher in 2014 than in 2008. Similarly, the contribution to the shallow aquifer in 2020 was 31 mm higher than in 2014. Likewise, in subbasin 33, the contribution to the shallow aquifer in 2014 was 50 mm higher than in 2008, and 40 mm higher in 2020 than in 2014. Figure 10 shows the increase in annual groundwater storage in both sub-basins.

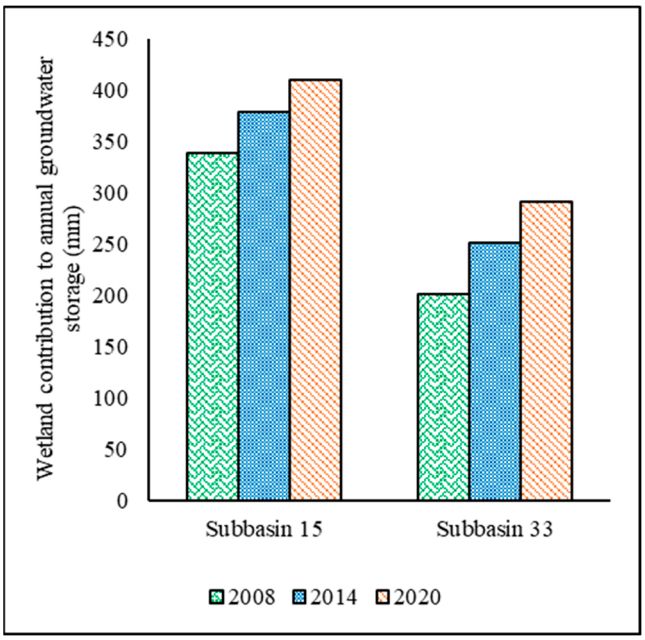

Figure 10. Effects of wetlands on annual shallow groundwater change.

On average, at the watershed level, the annual groundwater storage increase due to wetlands was 38 mm higher in 2020 than in 2008. Data from 101 randomly located groundwater monitoring wells were considered throughout the BSRW, based on maximum data availability from 2008 to 2020. The overall average groundwater level at BSRW in 2020 was 307 mm higher than in 2008. However, the overall aquifer decline was observed in the central region of the watershed (Figure 11), even though groundwater levels in northern and southern regions were generally not declining. Figure 11, obtained using the Kriging interpolation technique [68], shows the 12-year average alluvial aquifer changes from 2008 to 2020 based on randomly selected data from 101 monitoring wells. The central BSRW regions experienced average decreases of up to 176 mm per year. Therefore, despite the fact that wetlands have contributed to an increase in groundwater storage, water withdrawal

for irrigation in agricultural areas or other water uses may have resulted in a declining trend of the alluvial aquifer [69].

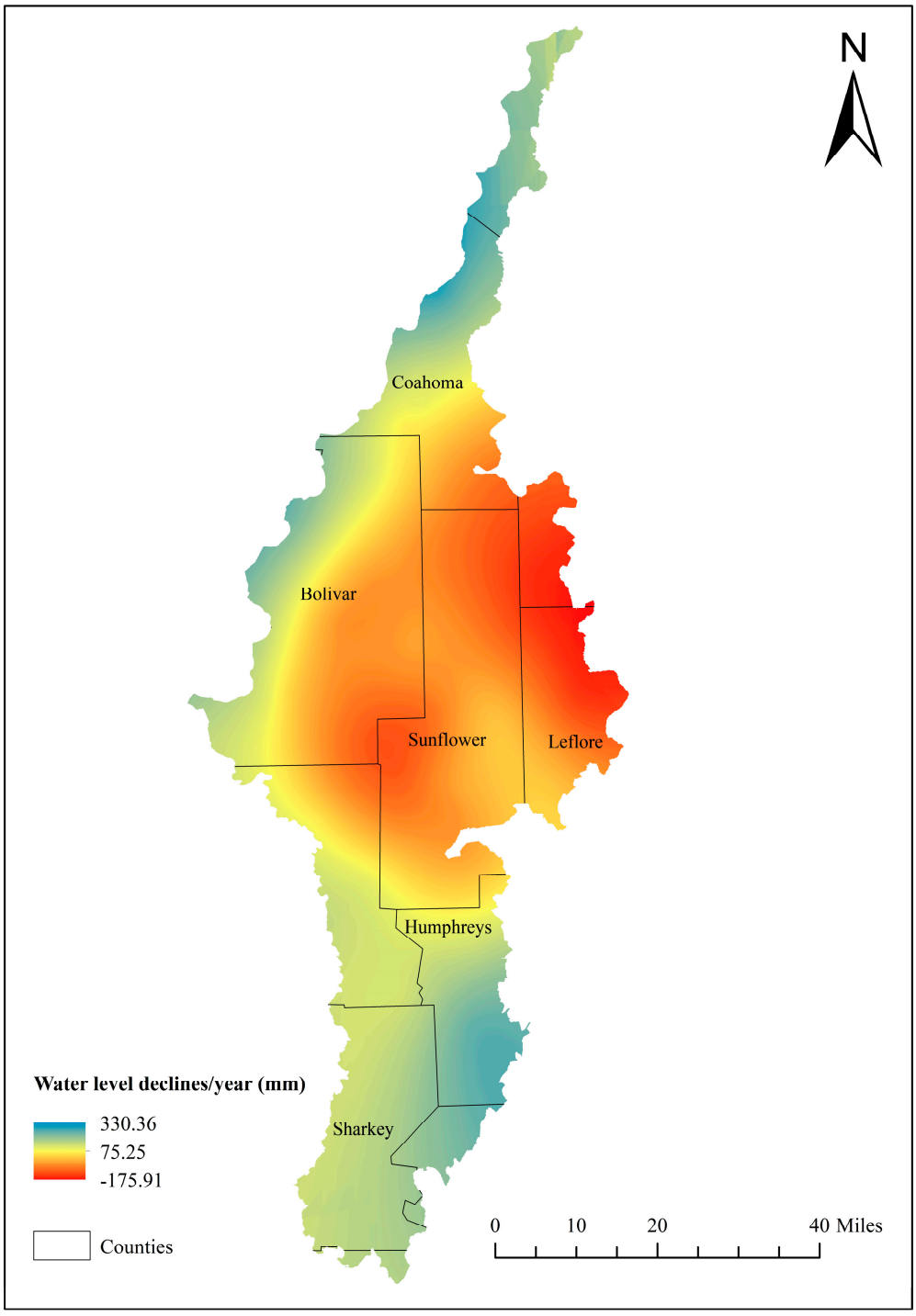

Figure 11. Twelve-year (2008–2020) variation in groundwater levels at watershed.

4. Discussion

4.1. Surface Water Quality

The SWAT model was calibrated and validated for streamflow, TSS, TP, and TN. The statistical measures R^2 and NSE were well above the criteria suggested by [70] during streamflow calibration and validation. Additionally, the statistics were compared to the comprehensive review article by [46]. To develop standard NSE and R^2 criteria for defining the model performance, [46] conducted a review of over 250 articles that reported

SWAT applications worldwide. Statistics suggested that model performance was satisfactory for streamflow simulation. In this study, model performances (NSE and R^2) during streamflow simulation were comparable to, or better than, the values obtained in previous studies [71–73]. Similarly, the statistics obtained during TSS calibration and validation were above the criteria suggested by [70]. The model can be considered satisfactory for monthly sediment simulation if R^2 is greater than 0.40 and NSE is greater than 0.45 [70]. Additionally, the performance of the model in simulating monthly sediment yield was deemed satisfactory when compared to other sediment modeling studies [74–76]. Likewise, acceptable model performance was achieved during the calibration and validation of TP. Slightly lower performance was estimated at Merigold station during the validation period. This is primarily due to underestimated loadings during storm events. A similar result was obtained in a previous study by [77] for the Cox Creek and Aldgate gauge stations during multisite calibration. Similarly, a low performance (R^2 = 0.38 and NSE = 0.08) of the model was obtained during monthly TP simulation in a study conducted by [78]. Despite the low performance, the prediction was better for the yearly simulation of TP. The low performance in our study may be due to the lack of incorporation of atmospheric deposition of phosphorus, septic loading, and non-agricultural fertilizer [79]. Additionally, the underestimation of TP load, such as in February 2018, resulted in lower performance. This may be the result of the dispersion of manure across a region and an abrupt washout following heavy precipitation and increased runoff. Similarly, during the validation of TN, the Merigold station exhibited the lowest performance. This was due to underestimated loads during high-flow events. In addition, this may be because nitrogen is volatile in nature and its concentrations vary greatly between HRUs within the same subbasin [44]. The results obtained are comparable to those of a previous study deploying a multisite calibration technique [77]. An earlier study by [80] at the BSRW also found that predicting nitrogen loads had the highest level of uncertainty as compared to streamflow and TSS with the highest NSE of 0.07 and the lowest of −0.09. The study further suggested that this uncertainty might even be larger during peak flow circumstances. A study by [78] also obtained low performance (R^2 = 0.27 and NSE = 0.16) during monthly nitrate loading simulation due to underestimated peak flow conditions. The simulated and measured annual nitrate loads revealed strong agreement, despite the model's low performance in predicting monthly nitrate loads.

4.2. Groundwater Level Change

The maximum value of the objective function, NSE, was achieved by setting the value of the specific yield of MRVAA to 0.21. Thus, the obtained value of the specific yield was close to the value of 0.26 obtained in the previous study by [42], and 0.17 obtained in the study by [52]. The usual range of specific yield in shallow aquifers is between 0.01 and 0.3 [81]. The obtained value was found to be within this range.

4.3. Effects of Wetland Areas

The streamflow and water quality reductions obtained in this study were compared to those of several previous studies to validate the reliability of the findings. Based on the results in two sub-basins, the areas of wetlands ranging from 1540 to 2657 ha contributed to the reduction of flow by 1 to 11%, TSS by 19 to 89%, TN by 10 to 43%, and TP by 8 to 44%. A study conducted by [31] simulated six different wetland restoration scenarios, where the wetland area from the year 1968 (2998 ha) was taken as the upper limit for restoration from the wetland area of 2379 ha in the year 2005. The average annual flow reduction was 1.6 to 23.4%, sediment yield was reduced by up to 16.9%, and the TN and TP reductions were obtained in the range of 2.4 to 23.4% at the watershed outlet. In another study by [82], the result showed that sediment could be reduced by 60 to 90% by riparian wetlands. Similarly, [83] reported annual sediment retention in wetlands could be up to 80%, similar to our findings. Previous research conducted by [84] used the APEX model at the sub-watershed scale to simulate ponds over areas ranging from 3426 to 14,082 ha. The

findings of the study showed that ponds were able to reduce runoff by 0 to 16%, sediment by 5 to 81%, TN by 4 to 80%, and TP by 3 to 52%. The reduction in flow, TSS, and TP in this study were comparable to the outcomes of [84]. Similarly, wetland restoration effects on water quality and quantity were simulated by [85] at a watershed scale. This study found that restoration of 460 to 550 ha of wetlands could increase the reduction of discharge by 20%, sediment by 25%, TN by 18%, and TP by 12%. In our study, in both the sub-basins, an increase in 349–406 ha of wetlands from 2008 to 2020 increased flow reduction by up to 2%, sediment reduction by up to 37%, TN reduction by up to 3%, and TP reduction by up to 13%. Likewise, the shallow groundwater storage contribution increased by 21% and 44% in sub-basins 15 and 33 due to an increase in wetlands from 2008 to 2020. A study by [29] simulated the effect of wetlands, and reported a 14% decrease in groundwater recharge and a 7% decrease in groundwater flow due to the loss of geographically isolated wetlands (GIWs). It has been attributed to the fact that decreased water interception due to the loss of GIWs increased runoff from land to streams, and decreased infiltration. The results of our study on the impacts of wetlands on flow, sediment, nitrogen, phosphorous, and groundwater storage were comparable to the range of values reported in earlier studies.

4.4. Study Limitations

This study utilized the USDA, NASS's CDL, to obtain the wetland areas within the watershed, and the results are dependent upon the land cover classification accuracy within the CDL. Similarly, the choice of parameter ranges for wetland simulation was based on the values used in previous studies. Field verification would support the validity of the outcomes. The study analyzed the effects of changing wetland areas on hydrological and water quality responses on only two subbasins of interest. While the study acknowledges its limitation of concentrating on only two subbasins, it nonetheless provides useful insights into increasing wetland areas over time within BSRW and their benefits in flow, sediment, and nutrient reductions, as well as groundwater recharge. To determine whether the resulting streamflow, water quality parameters, and groundwater storage due to wetlands vary greatly, this work may be carried out in more watersheds with various topography and soil types in the future.

5. Conclusions

This study evaluated the historical trend of wetland area changes from 2008 to 2020, and changes in their ecological benefits in terms of streamflow and water pollution reduction and groundwater storage increments. The LULC change analysis based in CDL provided by USDA, NASS, revealed that wetland areas increased in 38 out of 40 subbasins, except for subbasins 3 and 40 where they decreased by 0.03% and 0.64% of the subbasin areas, respectively. The maximum increase was 15% of the subbasin area at subbasin 7, and the minimum increase was 0.12% at subbasin 34. The average increase in wetlands was 3.5% of the subbasin area, with a standard deviation of 3.9%. The hydrologic and water quality responses were estimated for subbasins of interest (i.e., 15 and 33). Between 2008 and 2020, subbasins 15 and 33 experienced 15% and 26% increments in wetland areas, respectively. The increase in wetland areas resulted in an increase in flow reduction by between 1% and 2% from 2008 to 2020. Similarly, sediment reduction increased by between 3% and 37%, TP reduction increased by between 5% and 13%, and TN reduction increased by between 3% and 4%. Similarly, the contribution to shallow aquifer storage increased by 71 mm to 90 mm in 2020, compared to 2008. Even though the wetlands helped to increase groundwater storage in selected subbasins, the overall trend of the aquifer declined in the watershed's central part. This could be a result of increased water withdrawal for irrigation or other purposes.

The methodological framework used in this study may be beneficial for studying the temporal changes in the impacts of wetlands on hydrology and water quality. Similarly, this study highlights the importance of the conservation of wetlands, and serves as a useful resource for watershed managers and concerned planners.

Author Contributions: D.N.: conceptualization, methodology, and manuscript draft preparation. P.P.: conceptualization, methodology, and manuscript review. Y.O., F.T., N.W. and V.V.: manuscript review. All authors have read and agreed to the published version of the manuscript.

Funding: The authors would like to acknowledge the partial financial support from the NIFA/AFRI competitive grant award # 2017-67020-26375, and the Bagley College of Engineering at Mississippi State University.

Data Availability Statement: The original contributions presented in the study are included in the article.

Acknowledgments: The authors wish to acknowledge the United States Geological Survey (USGS) and all other collaborators for their support.

Conflicts of Interest: The authors declare no conflicts of interest.

References

1. Hassan, Z.; Shabbir, R.; Ahmad, S.S.; Malik, A.H.; Aziz, N.; Butt, A.; Erum, S. Dynamics of land use and land cover change (LULCC) using geospatial techniques: A case study of Islamabad Pakistan. *SpringerPlus* **2016**, *5*, 812. [CrossRef]
2. Mitsch, W.J.; Gosselink, J.G. The value of wetlands: Importance of scale and landscape setting. *Ecol. Econ.* **2000**, *35*, 25–33. [CrossRef]
3. Ekumah, B.; Armah, F.A.; Afrifa, E.K.A.; Aheto, D.W.; Odoi, J.O.; Afitiri, A.-R. Assessing land use and land cover change in coastal urban wetlands of international importance in Ghana using Intensity Analysis. *Wetl. Ecol. Manag.* **2020**, *28*, 271–284. [CrossRef]
4. Jogo, W.; Hassan, R. Balancing the use of wetlands for economic well-being and ecological security: The case of the Limpopo wetland in southern Africa. *Ecol. Econ.* **2010**, *69*, 1569–1579. [CrossRef]
5. Cowardin, L.M. *Classification of Wetlands and Deepwater Habitats of the United States, Fish and Wildlife Service*; US Department of the Interior: Washington, DC, USA, 1979; p. 3. Available online: https://pubs.usgs.gov/publication/2000109 (accessed on 25 August 2022).
6. National Research Council. *Wetlands: Characteristics and Boundaries*; National Academies Press: Washington, DC, USA, 1995. [CrossRef]
7. Padmanabhan, G.; Bengtson, M.L. Assessing the influence of wetlands on flooding. In *Wetlands Engineering & River Restoration*; American Society of Civil Engineers: Reston, VA, USA, 2001. [CrossRef]
8. Bullock, A.; Acreman, M. The role of wetlands in the hydrological cycle. *Hydrol. Earth Syst. Sci.* **2003**, *7*, 358–389. [CrossRef]
9. Johnston, C.A. Sediment and nutrient retention by freshwater wetlands: Effects on surface water quality. *Crit. Rev. Environ. Control* **1991**, *21*, 491–565. [CrossRef]
10. Camacho-Valdez, V.; Ruiz-Luna, A.; Ghermandi, A.; Berlanga-Robles, C.A.; Nunes, P.A.L.D. Effects of land use changes on the ecosystem service values of coastal wetlands. *Environ. Manag.* **2014**, *54*, 852–864. [CrossRef]
11. Worku, T.; Khare, D.; Tripathi, S.K. Modeling runoff–sediment response to land use/land cover changes using integrated GIS and SWAT model in the Beressa watershed. *Environ. Earth Sci.* **2017**, *76*, 550. [CrossRef]
12. Alexakis, D.D.; Grillakis, M.G.; Koutroulis, A.G.; Agapiou, A.; Themistocleous, K.; Tsanis, I.K.; Michaelides, S.; Pashiardis, S.; Demetriou, C.; Aristeidou, K.; et al. GIS and remote sensing techniques for the assessment of land use change impact on flood hydrology: The case study of Yialias basin in Cyprus. *Nat. Hazards Earth Syst. Sci.* **2014**, *14*, 413–426. [CrossRef]
13. Hwang, S.-A.; Hwang, S.-J.; Park, S.-R.; Lee, S.-W. Examining the relationships between watershed urban land use and stream water quality using linear and generalized additive models. *Water* **2016**, *8*, 155. [CrossRef]
14. Souza-Filho, P.W.M.; de Souza, E.B.; Júnior, R.O.S.; Nascimento, W.R., Jr.; de Mendonça, B.R.V.; Guimarães, J.T.F.; Dall'agnol, R.; Siqueira, J.O. Four decades of land-cover, land-use and hydroclimatology changes in the Itacaiúnas River watershed, southeastern Amazon. *J. Environ. Manag.* **2016**, *167*, 175–184. [CrossRef]
15. Day, J.W.; Shaffer, G.P.; Cahoon, D.R.; DeLaune, R.D. Canals, backfilling and wetland loss in the Mississippi Delta. *Estuar. Coast. Shelf Sci.* **2019**, *227*, 106325. [CrossRef]
16. Berkowitz, J.F.; Johnson, D.R.; Price, J.J. Forested Wetland hydrology in a large Mississippi river tributary system. *Wetlands* **2020**, *40*, 1133–1148. [CrossRef]
17. Nepal, D.; Parajuli, P.B. Assessment of Best Management Practices on Hydrology and Sediment Yield at Watershed Scale in Mississippi Using SWAT. *Agriculture* **2022**, *12*, 518. [CrossRef]
18. Clark, B.R.; Hart, R.M.; Gurdak, J.J. *Groundwater Availability of the Mississippi Embayment*; US Geological Survey: Reston, VA, USA, 2011. [CrossRef]
19. Day, J.W., Jr.; Ko, J.-Y.; Rybczyk, J.; Sabins, D.; Bean, R.; Berthelot, G.; Brantley, C.; Cardoch, L.; Conner, W.; Day, J.N.; et al. The use of wetlands in the Mississippi Delta for wastewater assimilation: A review. *Ocean Coast. Manag.* **2004**, *47*, 671–691. [CrossRef]
20. Cheng, F.Y.; Van Meter, K.J.; Byrnes, D.K.; Basu, N.B. Maximizing US nitrate removal through wetland protection and restoration. *Nature* **2020**, *588*, 625–630. [CrossRef] [PubMed]

21. Gratzer, M.C.; Davidson, G.R.; O'Reilly, A.M.; Rigby, J.R. Groundwater recharge from an oxbow lake-wetland system in the Mississippi Alluvial Plain. *Hydrol. Process.* **2020**, *34*, 1359–1370. [CrossRef]
22. Walton, R.; Chapman, R.S.; Davis, J.E. Development and application of the wetlands dynamic water budget model. *Wetlands* **1996**, *16*, 347–357. [CrossRef]
23. Ogawa, H.; Male, J.W. Simulating the flood mitigation role of wetlands. *J. Water Resour. Plan. Manag.* **1986**, *112*, 114–128. [CrossRef]
24. Feldman, A.D. HEC-1 flood hydrograph package. *Comput. Model. Watershed Hydrol.* **1995**, *119*, 150.
25. Konyha, K.D.; Shaw, D.T.; Weiler, K.W. Hydrologic design of a wetland: Advantages of continuous modeling. *Ecol. Eng.* **1995**, *4*, 99–116. [CrossRef]
26. Sun, G.; Riekerk, H.; Comerford, N.B. Comerford, Modeling the forest hydrology of wetland-upland ecosystems in Florida 1. *JAWRA J. Am. Water Resour. Assoc.* **1998**, *34*, 827–841. [CrossRef]
27. Arnold, J.G.; Srinivasan, R.; Muttiah, R.S.; Williams, J.R. Large area hydrologic modeling and assessment part I: Model development 1. *JAWRA J. Am. Water Resour. Assoc.* **1998**, *34*, 73–89. [CrossRef]
28. Bekele, E.G.; Demissie, M.; Lian, Y. Optimizing the placement of best management practices (BMPs) in agriculturally-dominated watersheds in Illinois. In Proceedings of the World Environmental and Water Resources Congress 2011: Bearing Knowledge for Sustainability, Palm Springs, CA, USA, 22–26 May 2011; pp. 2890–2900. [CrossRef]
29. Lee, S.; Yeo, I.-Y.; Lang, M.; Sadeghi, A.; McCarty, G.; Moglen, G.; Evenson, G. Assessing the cumulative impacts of geographically isolated wetlands on watershed hydrology using the SWAT model coupled with improved wetland modules. *J. Environ. Manag.* **2018**, *223*, 37–48. [CrossRef]
30. Liu, Y.; Yang, W.; Wang, X. Development of a SWAT extension module to simulate riparian wetland hydrologic processes at a watershed scale. *Hydrol. Process.* **2008**, *22*, 2901–2915. [CrossRef]
31. Yang, W.; Wang, X.; Liu, Y.; Gabor, S.; Boychuk, L.; Badiou, P. Simulated environmental effects of wetland restoration scenarios in a typical Canadian prairie watershed. *Wetl. Ecol. Manag.* **2010**, *18*, 269–279. [CrossRef]
32. Bieger, K.; Hörmann, G.; Fohrer, N. The impact of land use change in the Xiangxi Catchment (China) on water balance and sediment transport. *Reg. Environ. Change* **2015**, *15*, 485–498. [CrossRef]
33. Dao, N.K.; Tadashi, S. Impact of climate and land-use changes on hydrological processes and sediment yield—A case study of the Be River catchment, Vietnam. *Hydrol. Sci. J.* **2014**, *59*, 1095–1108. [CrossRef]
34. Ni, X.; Parajuli, P.B.; Ouyang, Y.; Dash, P.; Siegert, C. Assessing land use change impact on stream discharge and stream water quality in an agricultural watershed. *CATENA* **2021**, *198*, 105055. [CrossRef]
35. Zhu, C.; Li, Y. Long-term hydrological impacts of land use/land cover change from 1984 to 2010 in the Little River Watershed, Tennessee. *Int. Soil Water Conserv. Res.* **2014**, *2*, 11–21. [CrossRef]
36. USDA. CropScape—NASS CDL Program. USDA NASS, 2019. Available online: https://nassgeodata.gmu.edu/CropScape/ (accessed on 29 January 2021).
37. NRCS. Web Soil Survey—Home. 2012. Available online: https://websoilsurvey.sc.egov.usda.gov/App/HomePage.htm (accessed on 29 January 2021).
38. Arthur, J.K. *Hydrogeology, Model Description, and Flow Analysis of the Mississippi River Alluvial Aquifer in Northwestern Mississippi*; US Department of the Interior, US Geological Survey: Reston, VA, USA, 2001. [CrossRef]
39. Arnold, J.G.; Kiniry, J.R.; Srinivasan, R.; Williams, J.R.; Haney, E.B.; Neitsch, S.L. *Input/Output Documentation, Soil Water Assessment Tool*; Texas Water Resources Institute: College Station, TX, USA, 2012. Available online: https://swat.tamu.edu/media/69296/swat-io-documentation-2012.pdf (accessed on 25 August 2022).
40. Neitsch, S.L.; Arnold, J.G.; Kiniry, J.R.; Williams, J.R. *Soil and Water Assessment Tool Theoretical Documentation Version 2009*; Texas Water Resources Institute: College Station, TX, USA, 2011. Available online: https://swat.tamu.edu/media/99192/swat2009-theory.pdf (accessed on 25 August 2022).
41. Arnold, J.G.; Kiniry, J.R.; Srinivasan, R.; Williams, J.R.; Haney, E.B.; Neitsch, S.L. *SWAT 2012 Input/Output Documentation*; Texas Water Resources Institute: College Station, TX, USA, 2013. Available online: https://hdl.handle.net/1969.1/149194 (accessed on 25 August 2022).
42. Dakhlalla, A.O.; Parajuli, P.B.; Ouyang, Y.; Schmitz, D.W. Evaluating the impacts of crop rotations on groundwater storage and recharge in an agricultural watershed. *Agric. Water Manag.* **2016**, *163*, 332–343. [CrossRef]
43. Risal, A.; Parajuli, P.B. Evaluation of the Impact of Best Management Practices on Streamflow, Sediment and Nutrient Yield at Field and Watershed Scales. *Water Resour. Manag.* **2022**, *36*, 1093–1105. [CrossRef]
44. Venishetty, V.; Parajuli, P.B. Assessment of BMPs by Estimating Hydrologic and Water Quality Outputs Using SWAT in Yazoo River Watershed. *Agriculture* **2022**, *12*, 477. [CrossRef]
45. Williams, J.R.; Berndt, H.D. Sediment yield prediction based on watershed hydrology. *Trans. ASAE* **1977**, *20*, 1100–1104. [CrossRef]
46. Gassman, P.W.; Reyes, M.R.; Green, C.H.; Arnold, J.G. The soil and water assessment tool: Historical development, applications, and future research directions. *Trans. ASABE* **2007**, *50*, 1211–1250. [CrossRef]
47. Winchell, M.; Srinivasan, R.; Di Luzio, M.; Arnold, J. *ArcSWAT Interface for SWAT2012: User's Guide*; Blackland Research & Extension Center, Texas A&M AgriLife Blackland Research & Extension Center: Temple, TX, USA, 2013; pp. 1–464.
48. USGS. The National Map—Advanced Viewer. Nationalmap.Gov. 2019. Available online: https://apps.nationalmap.gov/viewer/ (accessed on 29 January 2021).

49. NOAA, National Oceanic and Atmospheric Administration. 2021. Available online: https://www.ncdc.noaa.gov/ (accessed on 5 February 2021).
50. TAMU. Global Weather Data for SWAT. Texas A&M University. 2020. Available online: https://swat.tamu.edu/data/ (accessed on 25 February 2022).
51. MSU MAFES. MAFES—Variety Trials. 2020. Available online: https://www.mafes.msstate.edu/variety-trials/includes/forage/about.asp (accessed on 25 February 2022).
52. Ni, X.; Parajuli, P.B. Evaluation of the impacts of BMPs and tailwater recovery system on surface and groundwater using satellite imagery and SWAT reservoir function. *Agric. Water Manag.* **2018**, *210*, 78–87. [CrossRef]
53. Runkel, R.L.; Crawford, C.G.; Cohn, T.A. Load Estimator (LOADEST): A FORTRAN program for estimating constituent loads in streams and rivers. In *Techniques and Methods*; Geological Survey: Reston, VA, USA, 2004. [CrossRef]
54. Niraula, R.; Kalin, L.; Srivastava, P.; Anderson, C.J. Identifying critical source areas of nonpoint source pollution with SWAT and GWLF. *Ecol. Model.* **2013**, *268*, 123–133. [CrossRef]
55. Yen, H.; Jeong, J.; Feng, Q.; Deb, D. Assessment of input uncertainty in SWAT using latent variables. *Water Resour. Manag.* **2015**, *29*, 1137–1153. [CrossRef]
56. Draper, N.R.; Smith, H. *Applied Regression Analysis*, 3rd ed.; John Wiley & Sons Inc.: New York, NY, USA, 1998; p. 26.
57. Nash, J.E.; Sutcliffe, J.V. River flow forecasting through conceptual models part I—A discussion of principles. *J. Hydrol.* **1970**, *10*, 282–290. [CrossRef]
58. Abbaspour, K.C. *Swat-Cup 2012, SWAT Calibration Uncertainty Program—A User Manual*; Swiss Federal Institute of Aquatic Science and Technology: Dübendorf, Switzerland, 2013.
59. Wu, K.; Johnston, C.A. Hydrologic comparison between a forested and a wetland/lake dominated watershed using SWAT. *Hydrol. Process.* **2008**, *22*, 1431–1442. [CrossRef]
60. Ikenberry, C.D.; Crumpton, W.G.; Arnold, J.G.; Soupir, M.L.; Gassman, P.W. Evaluation of existing and modified wetland equations in the SWAT model. *JAWRA J. Am. Water Resour. Assoc.* **2017**, *53*, 1267–1280. [CrossRef]
61. Wang, X.; Yang, W.; Melesse, A.M. Using hydrologic equivalent wetland concept within SWAT to estimate streamflow in watersheds with numerous wetlands. *Trans. ASABE* **2008**, *51*, 55–72. [CrossRef]
62. Almendinger, J.E.; Debjani, D.; Ahmadi, M.; Zhang, X.; Srinivasan, R. Constructing a SWAT Model of the St, Croix River Basin, Eastern Minnesota Western Wisconsin. 2015. Available online: https://npgallery.nps.gov/GetAsset/10ab6a21-d027-4380-b7fc-c5483b0592e4?/ (accessed on 25 August 2022).
63. Babbar-Sebens, M.; Barr, R.C.; Tedesco, L.P.; Anderson, M. Spatial identification and optimization of upland wetlands in agricultural watersheds. *Ecol. Eng.* **2013**, *52*, 130–142. [CrossRef]
64. Kim, H.; Parajuli, P.B. Impacts of reservoir outflow estimation methods in SWAT model calibration. *Trans. ASABE* **2014**, *57*, 1029–1042. [CrossRef]
65. Barlow, J.R.B.; Clark, B.R. *Simulation of Water-Use Conservation Scenarios for the Mississippi Delta Using an Existing Regional Groundwater Flow Model*; US Department of the Interior, US Geological Survey: Reston, VA, USA, 2011. [CrossRef]
66. Rostamian, R.; Jaleh, A.; Afyuni, M.; Mousavi, S.F.; Heidarpour, M.; Jalalian, A.; Abbaspour, K.C. Application of a SWAT model for estimating runoff and sediment in two mountainous basins in central Iran. *Hydrol. Sci. J.* **2008**, *53*, 977–988. [CrossRef]
67. Benaman, J.; Shoemaker, C.A. An analysis of high-flow sediment event data for evaluating model performance. *Hydrol. Process.* **2005**, *19*, 605–620. [CrossRef]
68. Oliver, M.A.; Webster, R. Kriging: A method of interpolation for geographical information systems. *Int. J. Geogr. Inf. Sci.* **1990**, *4*, 313–332. [CrossRef]
69. YMD. 2019. Available online: https://www.ymd.org/ (accessed on 28 September 2022).
70. Moriasi, D.N.; Gitau, M.W.; Pai, N.; Daggupati, P. Hydrologic and water quality models: Performance measures and evaluation criteria. *Trans. ASABE* **2015**, *58*, 1763–1785. [CrossRef]
71. Abbaspour, K.C.; Rouholahnejad, E.; Vaghefi, S.; Srinivasan, R.; Yang, H.; Kløve, B. A continental-scale hydrology and water quality model for Europe: Calibration and uncertainty of a high-resolution large-scale SWAT model. *J. Hydrol.* **2015**, *524*, 733–752. [CrossRef]
72. Arnold, J.; Muttiah, R.; Srinivasan, R.; Allen, P. Regional estimation of base flow and groundwater recharge in the Upper Mississippi river basin. *J. Hydrol.* **2000**, *227*, 21–40. [CrossRef]
73. Parajuli, P.B.; Nelson, N.O.; Frees, L.D.; Mankin, K.R. Comparison of AnnAGNPS and SWAT model simulation results in USDA-CEAP agricultural watersheds in south-central Kansas. *Hydrol. Process.* **2009**, *23*, 748–763. [CrossRef]
74. Choukri, F.; Raclot, D.; Naimi, M.; Chikhaoui, M.; Nunes, J.P.; Huard, F.; Hérivaux, C.; Sabir, M.; Pépin, Y. Distinct and combined impacts of climate and land use scenarios on water availability and sediment loads for a water supply reservoir in northern Morocco. *Int. Soil Water Conserv. Res.* **2020**, *8*, 141–153. [CrossRef]
75. El-Sadek, A.; Irvem, A. Evaluating the impact of land use uncertainty on the simulated streamflow and sediment yield of the Seyhan River basin using the SWAT model. *Turk. J. Agric. For.* **2014**, *38*, 515–530. [CrossRef]
76. White, K.L.; Chaubey, I. Sensitivity analysis, calibration, and validations for a multisite and multivariable SWAT model 1. *JAWRA J. Am. Water Resour. Assoc.* **2005**, *41*, 1077–1089. [CrossRef]

77. Shrestha, M.K.; Recknagel, F.; Frizenschaf, J.; Meyer, W. Assessing SWAT models based on single and multi-site calibration for the simulation of flow and nutrient loads in the semi-arid Onkaparinga catchment in South Australia. *Agric. Water Manag.* **2016**, *175*, 61–71. [CrossRef]
78. Chu, T.W.; Shirmohammadi, A.; Montas, H.; Sadeghi, A. Evaluation of the SWAT model's sediment and nutrient components in the Piedmont physiographic region of Maryland. *Trans. ASAE* **2004**, *47*, 1523–1538. [CrossRef]
79. Luscz, E.C.; Kendall, A.D.; Hyndman, D.W. High resolution spatially explicit nutrient source models for the Lower Peninsula of Michigan. *J. Great Lakes Res.* **2015**, *41*, 618–629. [CrossRef]
80. Dakhlalla, A.O.; Parajuli, P.B. Assessing model parameters sensitivity and uncertainty of streamflow, sediment, and nutrient transport using SWAT. *Inf. Process. Agric.* **2019**, *6*, 61–72. [CrossRef]
81. Freeze, R.A.; Cherry, J.A. *Groundwater*; Prentice-Hall Inc.: Englewood Cliffs, NJ, USA, 1979; Volume 7632, p. 604.
82. Singh, A.; Rudra, R.; Yang, W.H. Adapting SWAT for riparian wetlands in an Ontario watershed. In Proceedings of the 3rd International SWAT Conference, Zürich, Switzerland, 11–15 July 2005; pp. 123–131. Available online: https://swat.tamu.edu/docs/swat/conferences/2005/SWAT%20Book%203rd%20Conference.pdf (accessed on 25 August 2022).
83. Elder, J.F.; Goddard, G. *Sediment and Nutrient Trapping Efficiency of a Constructed Wetland Near Delavan Lake, Wisconsin, 1993–1995*; US Geological Survey: Reston, VA, USA, 1996. [CrossRef]
84. Tuppad, P.; Santhi, C.; Srinivasan, R.; Williams, J.R. Best Management Practice (BMP) Verification Using Observed Water Quality Data and Watershed Planning for Implementation of BMPs. TSSWCB Project 04-I8. 2009. Available online: https://www.tsswcb.texas.gov/sites/default/files/files/programs/nonpoint-source-managment/Completed%20Projects/04-18-FR-RICHLNDBMP-09-21-10.pdf (accessed on 25 August 2022).
85. Wang, X.; Shang, S.; Qu, Z.; Liu, T.; Melesse, A.M.; Yang, W. Simulated wetland conservation-restoration effects on water quantity and quality at watershed scale. *J. Environ. Manag.* **2010**, *91*, 1511–1525. [CrossRef]